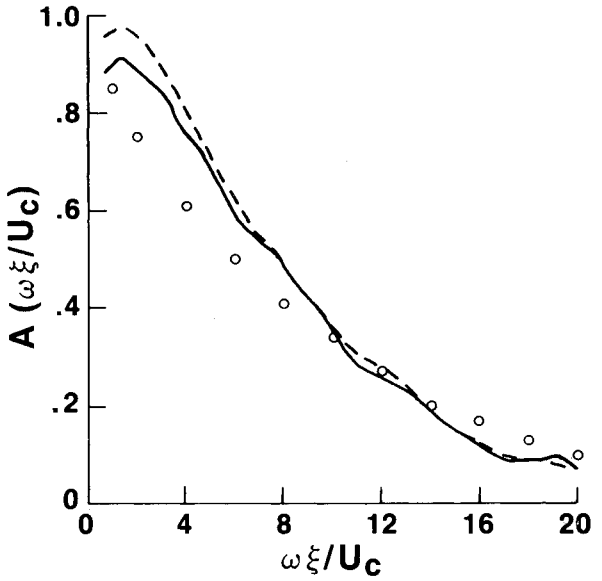

Fig. 4 Normalized longitudinal cross-spectral density $A(\omega\xi/U_c)$, $U_\infty = 20$ (ft/s), — = baseline, --- = riblets, o = results of Willmarth.[6]

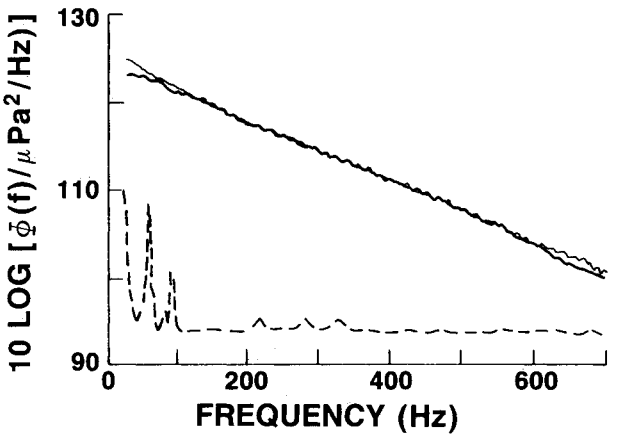

Fig. 5 Autospectral density $\Phi(f)$, $U_\infty = 10$ (ft/s), — = baseline, ▬ = riblets, --- = background noise.

spectra in Figs. 5 and 6 have not been corrected for spatial averaging. For the case of $R_\theta = 1.0 \times 10^4$, the attenuation (based on Corcos' correction) was 4.1 dB at 350 Hz and 10.7 dB at 700 Hz. For $R_\theta = 1.8 \times 10^4$, the attenuation was 4.1 dB at 800 Hz and 11.0 dB at 1600 Hz. The measured convection velocities were identical to within ±0.5% with those of the baseline measurements, shown in Fig. 2. A small but measureable increase in the magnitude of $A(\omega\xi/U_c)$ occurred at low values of $\omega\xi/U_c$, as shown in Figs. 3 and 4, with the effect being greater at the higher Reynolds number. Blake[7] measured a broadband decrease in the magnitude of $A(\omega\xi/U_c)$, a decrease in the convection velocities, and an increase in $\Phi(\omega)$ due to roughness elements, with heights on the order of 150 to 300 viscous lengths. He concluded that correlation distances were significantly reduced, due to the roughness elements. Blake's measurements qualitatively suggest that a reduction in drag due to skin friction would accompany an increase in the magnitude of $A(\omega\xi/U_c)$, as measured here. A limitation of this investigation is the lack of resolution of convected wave numbers with scales associated with the wall region of the turbulent boundary layer. Riblets may induce changes in these wave numbers that lead to changes in the levels of the autospectra at the associated frequencies. The results presented here show that the net contribution to the autospectra as well as the convection velocities from wave numbers associated with the outer region of the turbulent boundary layer is not significantly changed by the presence of riblets.

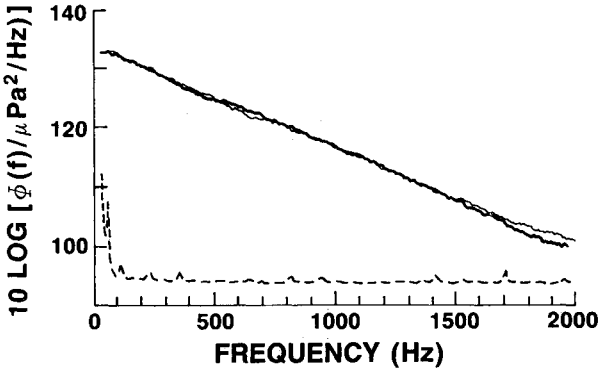

Fig. 6 Autospectral density $\Phi(f)$, $U_\infty = 20$ (ft/s), — = baseline, ▬ = riblets, --- = background noise.

Acknowledgments

Funding for this investigation was provided by the Naval Underwater Systems Center IR/IED Program, Job Order A70260. The author is grateful to Professor W. Willmarth at the University of Michigan for many helpful suggestions.

References

[1]Wilkinson, S. P., Anders, J. B., Lazos, B. S., and Bushnell, D. M., "Turbulent Drag Research at NASA Langley—Progress and Plans," *Proceedings of the Royal Aeronautical Society, Turbulent Drag Reduction by Passive Means,* London, Sept. 1987, pp. 1-32.

[2]Hama, F. R., *Society of Naval Architects Marine Engineers Transactions,* Vol. 62, 1954, p. 333-358.

[3]Corcos, G. M., "Resolution of Pressure in Turbulence," *Journal of the Acoustical Society of America,* Vol. 35, Feb. 1963, pp. 192-199.

[4]Bakewell, H. P., Jr., Carey, G. F., Schloemer, H. H., and Von Winkle, W. A., "Wall Pressure Correlations in Turbulent Pipe Flow," USL Rept. No. 559, 1-052-00-00, Naval Underwater Systems Ctr., New London, CT, 1962.

[5]Smol'yakov, A. V. and Tkachenko, V. M., *The Measurement of Turbulent Fluctuations,* Springer-Verlag, New York, 1983, pp. 32-35.

[6]Willmarth, W. W., "Pressure Fluctuations Beneath Turbulent Boundary Layers," *Annual Review of Fluid Mechanics,* Vol. 7, 1975, pp. 13-39.

[7]Blake, W. K., "Aero-Hydroacoustics for Ships," DTNSRDC-84/010, U.S. Government, Dept. of the Navy, Bethesda, MD, Vol. 2, 1984.

Calculation of Asymmetric Vortex Separation on Cones and Tangent Ogives Based on a Discrete Vortex Model

Suei Chin* and C. Edward Lan†
University of Kansas, Lawrence, Kansas
and
Thomas G. Gainer‡
NASA Langley Research Center, Hampton, Virginia

Introduction

DISCRETE line vortices have been used in the past to model symmetric[1,2] and asymmetric[3] vortx separations at zero sideslip in the leeward side of a body. In these

Received Sept. 26, 1988; revision received April 7, 1989.

*Graduate Research Assistant. Student Member AIAA.

†Professor, Department of Aerospace Engineering. Associate Fellow AIAA.

‡Aerospace Engineer.

investigations, a stagnation condition was imposed at the separation line. Other methods for predicting the asymmetric vortex shedding include the vortex cloud method[4] and solving the complete Navier-Stokes equations.[5] To obtain an asymmetric solution, Mendenhall et al.[4] introduced a perturbation to modify the predicted symmetric separation points to become asymmetric. In solving the complete Navier-Stokes equations for a cone-cylinder body,[5] asymmetry in the flowfield was introduced through asymmetric numerical truncation errors. But the computed side force was found too small.

In the present study, the boundary value problem for vortex separation at zero sideslip on cones and tangent ogives is set up by using a discrete vortex model. It is shown that the nonlinear algebraic equations for the boundary value problem admit multiple solutions which are physically feasible, including symmetric and asymmetric vortex solutions. One purpose of the present study is to offer the idea of multiple solutions as an alternative explanation of the existence of asymmetric vortex separation at zero slideslip. Note that vortex separation on a cylindrical afterbody is not treated.

Mathematical Model

Slender body theory is assumed applicable. For cones, the flow is assumed to be conical, so that the separation lines are straight lines, OS_1 and OS_2 (see Fig. 1). To treat a nonconical flow, a body is divided into many axial stations. Between two stations, flow properties are assumed to vary linearly (i.e., $\partial\Gamma/\partial x = \Delta\Gamma/\Delta x$, etc.). The separation lines are specified by their angular coordinates θ_1 and θ_2. Assuming that the locations of separation lines are known from experiment or boundary-layer calculations, the flow problem is then defined by the following conditions.

1) Separation-point condition: the total velocity at a separation point is equal to a mean tangential velocity (V_{tm}):

$$V_{tm} = \mathrm{Im}\left\{-e^{i\theta_1}\frac{dW}{dZ}\right\} \quad \text{at } Z = ae^{i\theta_1} \tag{1a}$$

$$V_{tm} = \mathrm{Im}\left\{e^{i\theta_2}\frac{dW}{dZ}\right\} \quad \text{at } Z = ae^{i\theta_2} \tag{1b}$$

2) Vortex force-free condition: the Kutta-Joukowski force acting on the vortex is zero,

$$-i\rho\Gamma_k\left[\lim_{Z\to Z_k}\left(\overline{\frac{dW}{dZ}} - \frac{\Gamma_k}{2\pi i}\frac{1}{Z-Z_k}\right) - V_\infty\frac{dZ_k}{dx}\right] = 0$$

$$k = 1,2 \tag{2}$$

where $Z = y + iz$, Γ is the vortex strength, and the overbar denotes complex conjugate. In Eqs. (1) and (2), the complex potential in the crossflow plane can be written as

$$W = iV_\infty \sin\alpha\left(Z - \frac{a^2}{\bar{Z}}\right) + V_\infty \cos\alpha\, a\frac{da}{dx}\ln Z$$

$$+ \frac{\Gamma_1}{2\pi i}\ln\frac{Z-Z_1}{Z-(a^2/\bar{Z}_1)} - \frac{\Gamma_2}{2\pi i}\ln\frac{Z-Z_2}{Z-(a^2/\bar{Z}_2)} \tag{3}$$

where $\bar{Z}$ is the complex conjugate of Z. The second term in Eq. (3) is a source term representing the effect of body geometric expansion.

It was shown in Ref. 6 that if V_{tm} in Eqs. (1) was set to 0 as it was done in Ref. 3, or to the expression derived by Smith,[7] the calculated vortex core positions were not accurate. A new expression for V_{tm} can be derived by considering the relationship between the rate of vortex shedding and the velocity (U_e) at the boundary layer edge[4]:

$$\partial\Gamma/\partial t = KU_e^2/2 \tag{4}$$

where K is an empirical factor used to reduce the strength of the primary shed vorticity due to counter-rotating secondary vortices.[8] If the average tangential velocity at the separation point (V_{tm}) is taken to be

$$V_{tm} = fU_e \tag{5}$$

and $\partial/\partial t$ is replaced by $(V_\infty \cos\alpha)\partial/\partial x$, Eq. (4) can be solved for V_{tm} to result in

$$V_{tm} = f[(2V_\infty \cos\alpha/K)(\Delta\Gamma/\Delta x)]^{1/2}$$

$$= f(2V_\infty \sin\alpha/K^{1/2})[\pi\Delta(a\gamma)/\Delta x \tan\alpha]^{1/2} \tag{6}$$

where γ is a dimensionless vortex strength defined by

$$\gamma = \Gamma/(2\pi a V_\infty \sin\alpha) \tag{7}$$

Note that for a cone,

$$\Delta(a\gamma)/\Delta x = \gamma a/x = \gamma \tan\delta \tag{8}$$

In the present applications, $K = 0.6$ as used in Ref. 4 and $f = 0.61$ as indicated in experimental data[9] for the vortex convection speed in a shear layer. In Smith's model, $K = 1.0$ and $f = 0.5$.[7] The present model produced more accurate vortex characteristics than Smith's as shown in Ref. 6.

By separating Eq. (2) into real and imaginary parts, and together with Eqs. (1), there are six nonlinear algebraic equations for six unknowns: γ_1, γ_2, y_1, z_1, y_2, and z_2. These results are then used in a contour integration for the local sectional coefficients of normal and side forces. The total force coefficients can be obtained by integrating the sectional coefficients over intervals of axial stations. Details can be found in Ref. 6.

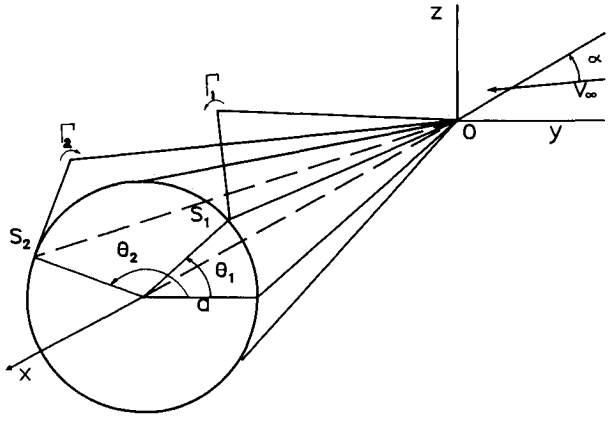

Fig. 1 Coordinate system.

Results and Discussion

A numerical scheme based on Broyden's modified Newton's method[10] is used to solve the system of nonlinear algebraic equations. Typically, the first-branch solution (symmetric if separation lines are symmetrical) can be easily obtained. In search of additional solutions, a function deflation technique[11] is needed to avoid convergence to the first branch again. For the present purposes, the separation lines will be assumed symmetrical unless otherwise noted. Their locations are calculated from empirical equations given in Ref. 12 for cones and those in Ref. 13 for tangent ogives in a laminar flow. Typically, the asymmetric solution starts at an axial location aft of where the symmetric one begins.[6]

The calculated side force coefficients (C_y, based on the base area) for a cone and a tangent ogive are compared with data in

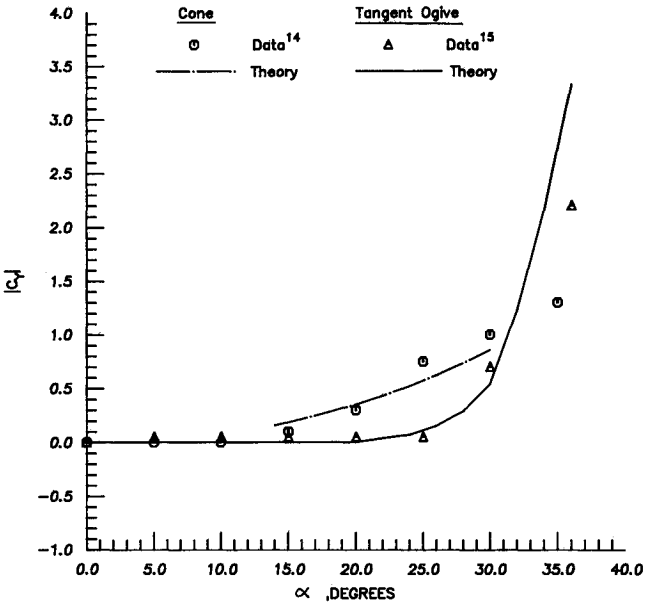

Fig. 2 Side-force coefficients for an 8 deg cone and a tangent ogive with a fineness ratio of 5.

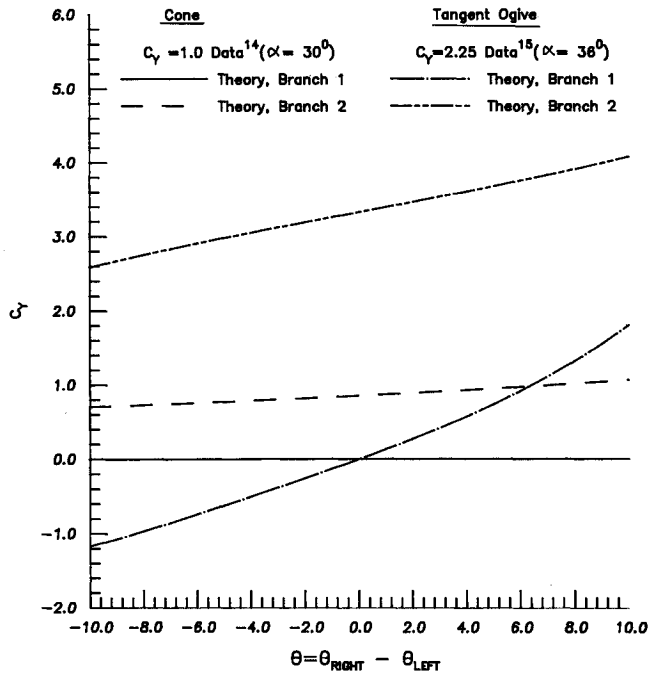

Fig. 3 Effect of asymmetric separation points on side-force coefficients for an 8 deg cone at $\alpha = 30$ deg and for a tangent ogive with a fineness ratio of 5 at $\alpha = 36$ deg.

Fig. 2. It is seen that the predicted C_y is reasonably accurate. More calculated results showing the same trend can be found in Ref. 6.

The main interest here is to see how the calculated C_y is are affected if separation locations are not symmetrical. To illustrate, the left separation location is kept fixed at the value used in the symmetric case ($\theta = 141.96$ deg for the cone and an average of 154 deg for the tangent ogive), and the right separation point is shifted up ($+\Delta\theta$) and down ($-\Delta\theta$) to obtain asymmetry of separation points. Again, two branches of solution can be calculated. The second-branch solution for the cone produces correct C_y values (Fig. 3), but not the first-branch solution. On the other hand, to produce an experimental C_y of 2.25 at $\alpha = 36$ deg based on the first-branch solution for the tangent ogive, the right separation point must be shifted up by about 12 deg, which may not be realistic on an ogive section. Based on the second-branch solution, C_y is overpredicted as it is also indicated in Fig. 2 at high α, probably because the fineness ratio is not large enough for the slender-body theory to be accurate. Based on these results, it is possible that measured side-force coefficients can only be predicted by second-branch solutions. It should be noted that although the present method does not predict the triggering mechanisms of flow asymmetry, it provides a way to calculate the maximum possible side force at zero sideslip.

Conclusions

Based on a discrete vortex model, two branches of solution to the boundary-value problem of vortex separation on a cone and a tangent ogive were shown to exist. The asymmetric solutions for the cone and the tangent ogive were shown to produce side-force coefficients at zero sideslip consistent with available data. It was also shown that the first-branch solution could not produce large enough side-force coefficients as measured in experiment for a cone.

Acknowledgment

This work was supported by NASA Grant NGS-1629 for the first two authors.

References

[1]Bryson, A. E., "Symmetrical Vortex Separation on Circular Cylinders and Cones," *Journal of Applied Mechanics,* Vol. 26, 1959, pp. 643-648.

[2]Schindel, L. H., "Effects of Vortex Separation on the Lift Distribution on Bodies of Elliptic Cross Section," *Journal of Aircraft,* Vol. 6, 1969, pp. 537-543.

[3]Dyer, D. E., Fiddes, S. P., and Smith, J. H. B., "Asymmetric Vortex Formation from Cones at Incidence—A Simple Inviscid Model," *Aeronautical Quarterly,* Nov. 1982, pp. 293-312.

[4]Mendenhall, M. R. and Perkins, S. C., Jr., "Vortex Cloud Model for Body Vortex Shedding and Tracking," *Progress in Astronautics and Aeronautics: Tactical Missile Aerodynamics,* Vol. 104, edited by Hemsch, M. J, and Nielsen, J. N., AIAA, New York, 1986, pp. 519-571.

[5]Graham, J. E. and Hankey, W. L., "Computation of the Asymmetric Vortex Pattern for Bodies of Revolution," *AIAA Journal,* Vol. 21, Nov. 1983, pp. 1500-1504.

[6]Chin, S. and Lan, C. E., "Calculation of Symmetric and Asymmetric Vortex Separation on Cones and Tangent Ogives Based on Discrete Vortex Models," NASA CR-4122, Feb. 1988.

[7]Smith, J. H. B., "Inviscid Fluid Models, Based on Rolled-up Vortex Sheets, for Three-Dimensional Separation at High Reynolds Number," Paper No. 9, AGARD-LS-94, 1978.

[8]Wardlaw, A. B. Jr., "High-Angle-of-Attack Missile Aerodynamics," AGARD-LS-98, 1979.

[9]Patel, M. H., "The Delta Wing in Oscillatory Gusts," *AIAA Journal,* Vol. 18, May 1980, pp. 481-486.

[10]Broyden, C. G., "A Class of Methods for Solving Nonlinear Simultaneous Equations," *Mathematics of Computation,* Vol. 19, 1965, pp. 577-593.

[11]Brown, K. M., "Computer Oriented Algorithms for Solving Systems of Simultaneous Nonlinear Algebraic Equations," *Numerical Solution of System of Nonlinear Algebraic Equations,* edited by G. D. Byrne and C. A. Hall, Academic, 1973.

[12]Friberg, E. G., "Measurement of Vortex Separation, Part II: Three-Dimensional Circular and Elliptic Bodies" MIT Aero. Lab. TR 115, 1965.

[13]Schindel, L. H. and Chamberlain, J. E., "Vortex Separation on Slender Bodies of Elliptic Cross Section," MIT Aero. Lab. TR 138, 1967.

[14]Coe, P. L., Jr., Chambers, J. R., and Letko, W., "Asymmetric Lateral-Directional Characteristics of Pointed Bodies of Revolution at High Angles of Attack," NASA TN D-7095, 1973.

[15]Keener, E. R., Chapman, G. T., Cohen, L., and Taleghani, J., "Side Forces on Forebodies at High Angles of Attack and Mach Numbers from 0.1 to 0.7: Two Tangent Ogives, Paraboloid and Cone," NASA TMX-3438, Feb. 1977.